Federal Aviation Administration

DOT/FAA/AM-23/17
Office of Aerospace Medicine
Washington, DC 20591

Seat and Occupant Response in Energy Absorbing Seats

Amanda M. Taylor
David M. Moorcroft

Civil Aerospace Medical Institute
Federal Aviation Administration
Oklahoma City, OK 73169

June 2023

NOTICE

This document is disseminated under the sponsorship of the U.S. Department of Transportation in the interest of information exchange. The United States Government assumes no liability for the contents thereof.

This publication and all Office of Aerospace Medicine technical reports are available in full-text from the Civil Aerospace Medical Institute's publications website (www.faa.gov/go/oamtechreports) and at the National Transportation Library's Repository & Open Science Access Portal (https://rosap.ntl.bts.gov/)

Technical Report Documentation Page

1. Report No.	2. Government Accession No.	3. Recipient's Catalog No.
DOT/FAA/23/17		

4. Title and Subtitle	5. Report Date
Seat and Occupant Response in Energy Absorbing Seats	June 2023
	6. Performing Organization Code AAM-632

7. Author(s)	8. Performing Organization Report No.
Taylor, Amanda M. (ORCID 0000-0002-1466-0857) Moorcroft, David M. (ORCID 0000-0002-9709-1150)	

9. Performing Organization Name and Address	10. Work Unit No. (TRAIS)
FAA Civil Aerospace Medical Institute P.O. Box 25082 Oklahoma City, OK 73125	11. Contract or Grant No.

12. Sponsoring Agency name and Address	13. Type of Report and Period Covered
Office of Aerospace Medicine Federal Aviation Administration 800 Independence Ave., S.W. Washington, DC 20591	Technical Report
Office of Aerospace Medicine Federal Aviation Administration	14. Sponsoring Agency Code

15. Supplemental Notes

The research was accomplished using FAA RE&D funding programmed through the aeromedical research budget (project # A11J.RS.3). This research underwent peer review. Project Sponsor: Joseph Pellettiere, Technical report
DOI: https://doi.org/10.21949/1524450.
Author roles: Taylor (Data Collection, Data Analysis, & Report Writing) Moorcroft: (Data Collection, Data Analysis & Report Writing).
Data available at: https://www.nhtsa.gov/research-data/research-testing-databases#/biomechanics

16. Abstract

The Federal Aviation Administration (FAA) has undertaken research programs to support streamlining various facets of the seat certification process. Previous research evaluated potential methods to qualify replacement of worn seat cushions used in low G applications (Part 25 and Part 23 passenger) and better quantify variability in vertical testing. The current research focused on higher energy rotorcraft environment where seating systems have energy absorption built in to reduce an occupant's risk of spinal injury. To gain a better understanding of how a seat with energy absorption characteristics behaves during a vertical test, the FAA's Civil Aerospace Medical Institute (CAMI) tested two seats with different styles of energy absorption: motion of the seat relative to the frame and buckling of the bottom of the seat only. Additionally, a simplified rigid seat test was used to evaluate whether the recorded seat pan acceleration of a stroking seat can be applied to the entire sled and provide similar occupant response to the original test. The stroking seat absorbed energy by creating a phase shift between the lumbar load and the sled deceleration. The buckling seat acted as a load limiter. Both methods of energy absorption reduced the measured lumbar load to below the magnitude expected from a fixed, rigid seat. For the rigid seat test, magnitude and phase differences between the original test and the simplified test suggest that this method may not be a suitable replacement for a full-scale test. Combining these results with those from projects focused on Part 23 and Part 25 conditions, a simplified method of cushion replacement for Part 27/29 rotorcraft is not recommended at this time.

17. Key Words	18. Distribution Statement
Energy Absorbing Seats, Lumbar Load, Seat Pan Acceleration	Document is available to the public through the National Transportation Library: https://ntl.bts.gov/ntl

19. Security Classif. (of this report)	20. Security Classif. (of this page)	21. No. of Pages	22. Price
Unclassified	Unclassified	30	

Form DOT F 1700.7 (8-72) Reproduction of completed page authorized

ACKNOWLEDGMENTS

Research reported in this paper was conducted under the sponsorship of the FAA Office of Aircraft Certification Service and was accomplished by the Aerospace Medical Research Division, Protection and Survival Research Branch, Engineering Sciences Section, Biodynamics Research Team (AAM-632), at the FAA Civil Aerospace Medical Institute. This work was performed under RE&D control account number A11J.RS.3.

The work would be unable to be completed without the full support of the technical staff at CAMI, Jeff Ashmore, Jim Biegler (contractor for Cherokee CRC), David DeSelms, Ian Hellstrom, Jesse Kindler (contractor, Venesco, LLC), and Ronnie Minnick.

We also thank East/West Industries and GippsAero for collaborating with us on this research by providing crashworthy seats.

Table of Contents

List of Figures

List of Tables

Seat and Occupant Response in Energy Absorbing Seats

BACKGROUND

Seating systems in aircraft and rotorcraft require two dynamic tests at different levels of acceleration and duration based on the specific installation (Emergency Landing Dynamic Conditions, 2017 14 C.F.R. §25.562, 2022; 14 C.F.R. §27.562, 2022; 14 C.F.R. §29.562; 2022). One of the two tests required is a primarily vertical impact with a minimum impact velocity of 30 ft/sec, peak acceleration of 30 G, and an impact angle of 30° off vertical for rotorcraft (Part 27 and 29). For small aircraft (Part 23), the minimum impact velocity of 31 ft/sec and the peak acceleration must be at least 19 G for pilot seats and 15 G for passenger seats. In this test, the principal occupant protection measurement is the compressive load in the lumbar spinal column, which has a regulatory limit of 1500 lb and requires the use of the Hybrid II Anthropomorphic Test Device (ATD), or its equivalent, sitting in the normal upright position. Any major alteration to the seating system components can require retesting to show that the alteration did not increase the injury potential for the occupant. In the vertical direction, the seat bottom cushion plays a vital role in controlling the lumbar load of the occupant and ensuring that the occupant interacts with the seating structure as designed. If the manufacturer simply changes out the cushion and replaces it with an identical part composed of the original materials to the original dimensions, no additional testing is required. If, however, there were a desire to change the cushion for something of a different dimension or composition, retesting would be required. Manufacturers have expressed interest in a means of changing the seat cushion bottom that is simpler and more cost-effective while maintaining the level of safety.

The Federal Aviation Administration (FAA) has undertaken research programs to support streamlining various facets of the seat certification process. Component testing of seat cushion foams yielded an FAA policy for replacing monolithic cushions for Part 25 installations (Hooper & Henderson, 2005; Federal Aviation Administration, 2005). Additional research was conducted to determine if rigid seat testing could serve as an alternative to multi-layer cushions made of various foam materials and to more accurately quantify variability in vertical testing (DeWeese, Moorcroft, & Taylor, 2021; Taylor, Moorcroft, & DeWeese, 2017; Moorcroft, DeWeese, & Taylor, 2010. After numerous tests, no definitive trend was identified between the performance of a cushion on a real seat and that of the same cushion type on a rigid seat. Consequently, the findings suggest that, at present, the seat and cushion must be evaluated as a combined system.

Part 27 and 29 operate in a higher energy rotorcraft environment, and the seating systems have energy absorption built in to reduce an occupant's risk of spinal injury. Based on the knowledge gained in the research focused on the Part 23 and Part 25 environments, a better understanding of how a seat with energy absorption characteristics behaves during a vertical test is required before any cushion replacement methodology may be considered.

METHODS

To meet the occupant injury limits, rotorcraft seats must be designed to attenuate energy. Additionally, due to the configuration of the cabins, the seats may be mounted either to the floor of the aircraft or to the bulkhead. To evaluate these parameters, three seats and two different installation types were tested, focusing on the loads transmitted to the occupant and structure. Two energy absorption styles were tested: the seat's motion relative to the

frame and buckling of the bottom of the seat only. The two types of mounting are bulkhead-mounted and floor-mounted.

Seat Types

Bulkhead-Mounted Seat

A bulkhead-mounted seat (Figure 1) mounts to the aircraft's bulkhead or internal sidewall. The test article was made of a seat bucket attached to rails affixed to a rigid frame with an interchangeable metallic strap energy absorber. During vertical loading, the seat bucket moves along the rails relative to the frame, and the straps deform, absorbing the energy of the crash. The restraint system was a four-point belt attached directly to the seat bucket instead of the aircraft.

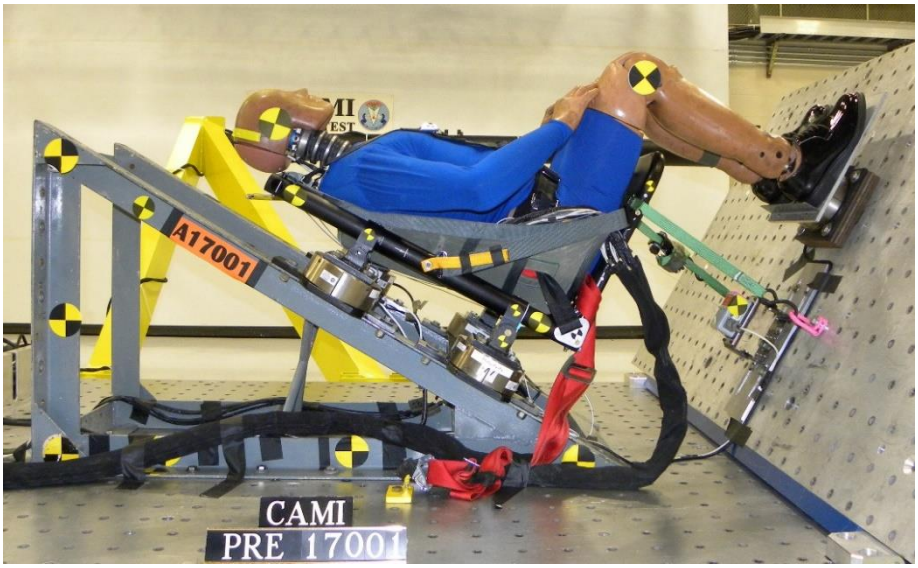

Figure 1: Bulkhead-mounted seat

Floor-Mounted Seat

A floor-mounted seat is mounted directly to the floor of the aircraft (Figure 2). The test article was made primarily of folded, thin-walled metal making it very light. The bottom box structure buckles during vertical loading, acting as a load limiter. The restraint system was a three-point belt with the shoulder belt attachment point on the side of the aircraft. A drawing of the installation was used to fabricate an anchor point to reflect the correct shoulder belt geometry.

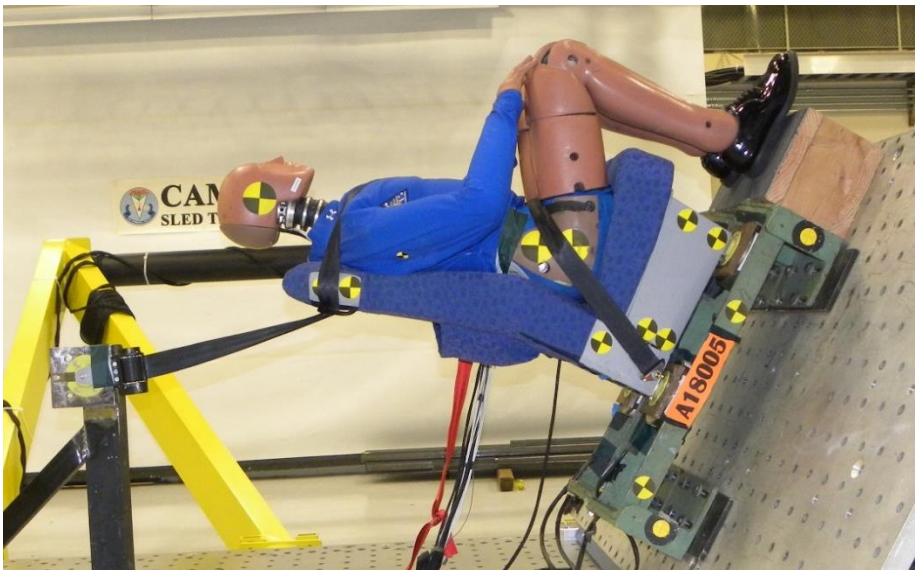

Figure 2: Floor-mounted seat

Rigid Seat

A simplified rigid seat test was used to evaluate whether a stroking seat's recorded seat pan acceleration can be applied to the entire sled and provide a similar occupant response to the original test (Figure 3). The original test, from 1980, was from a military helicopter seat with a rigid shell, a proprietary cushion of unknown composition, and a four-point belt. The test had a 40 G peak deceleration and greater than 10 inches of stroke. The simplified rigid seat had a back angle of 13° with respect to vertical, a flat seat pan with an angle of 5° with respect to horizontal, and a lapbelt anchored in a way that facilitated seating of the ATD. Because the original seat cushion was unavailable, two common aircraft seat cushion foams were tested to account for the uncertainty of the cushion response. The first was a four-inch monolithic midrange Dax® Firehard foam, Dax 47, with an indentation load deflection of 40 to 50 lbs. The second was a two-inch monolithic rate-sensitive foam, Confor™ 45 AC, with an indentation load deflection of 48 lb (Skandia Inc., n.d.). Although the two foams have similar indentation load deflection values, the Dax is open-celled and is fairly rate insensitive, while the Confor is closed-cell and highly rate sensitive.

The seat back position of the rigid seat was adjusted by adding a cloth-covered, closed cell foam shim so that the ATD pelvis was in the same fore/aft position relative to the pan-back intersection as when seated in the nominal 1-G seated position. A floor was included for realistic force distribution between the pelvis and the feet. The simulated floor used with the rigid seat was adjusted so that the distance between the hip point (H-point) and the center of the ankle was the same as the 1-G seated position, approximately 13 inches. The H-point of the ATD lies on a line passing through the center of both hip ball and socket joints of the ATD.

Figure 3: Rigid seat

Test Device

The ATD used to assess injury risk was a 50th percentile-sized male FAA Hybrid III, a modification of the automotive Hybrid III to incorporate parts of the Hybrid II to make it useable for vertical testing (Gowdy et al., 1999).

ATD Seating Method

The nominal upright ATD seated position (1-G position) was determined with respect to rigid points on each seat while the seats were mounted in the horizontal configuration (Figure 4). For this measurement, the ATD was seated according to a procedure developed at the Civil Aerospace Medical Institute (CAMI) that resulted in a consistent fore/aft position and initial pelvis angle (Moorcroft, DeWeese, & Taylor, 2010). This procedure involves suspending the ATD above the seat cushion approximately one inch. A rigid bar is inserted under the thighs just aft of the knees and used to elevate them slightly to avoid interfering with the ATD self-aligning. A force gauge is used to press on the sternum of the ATD with approximately 20 lb of force while the ATD is lowered into full contact with the seating surface. The ATD is rocked from side-to-side and allowed to sit for five minutes to settle into the seat. This settling time is necessary for the Confor to contour to the pelvis of the ATD fully. A surrogate wooden seat with pan and back angles identical to the metal seat was used for the rigid seat (Figure 5). The origin selected for the seating was the intersection of the rigid seat pan and seat back, which could be easily located on both the rigid test seat and the wooden surrogate.

A three-dimensional coordinate measuring machine was used to record the ATD head center of gravity (Head CG) photometric target and H-Point and vertical pelvis targets. The torso angle was derived using the H-Point and Head CG; the pelvis angle was derived using the H-Point and the vertical pelvis target. Once the seats were pitched up, the ATD was pushed into the seat cushion until the H-Point, pelvis angle, and torso angle matched the 1-G position within a tolerance (Moorcroft, DeWeese, & Taylor, 2010).

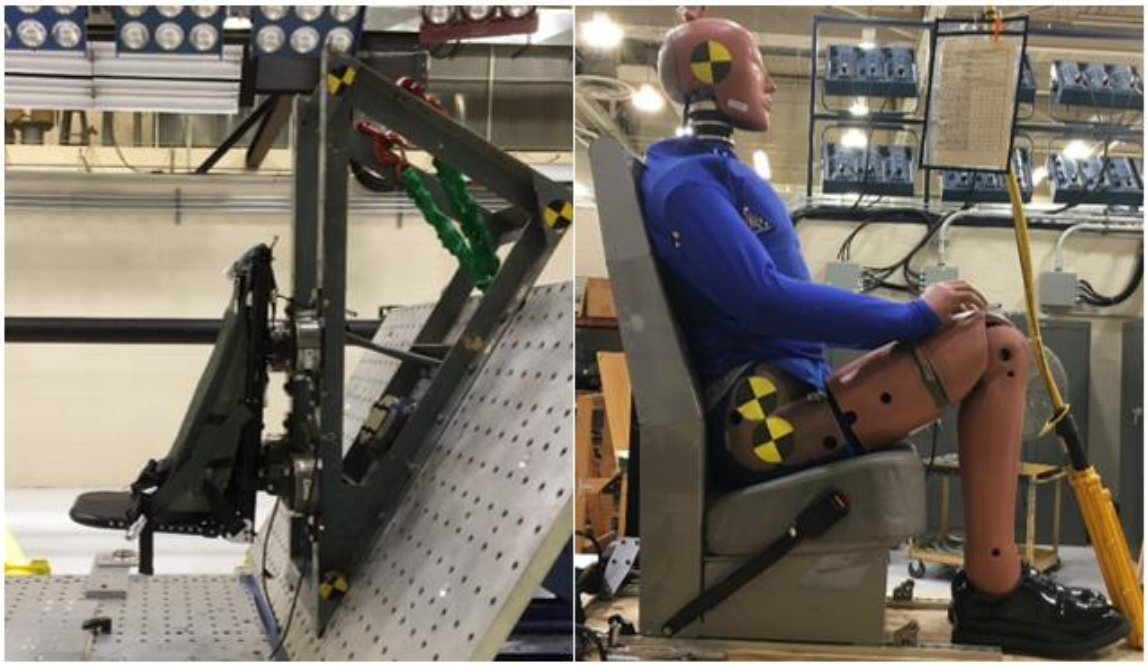

Figure 4: Bulkhead-mounted seat (left) and floor-mounted seat (right) in the configuration for 1-G seating procedure

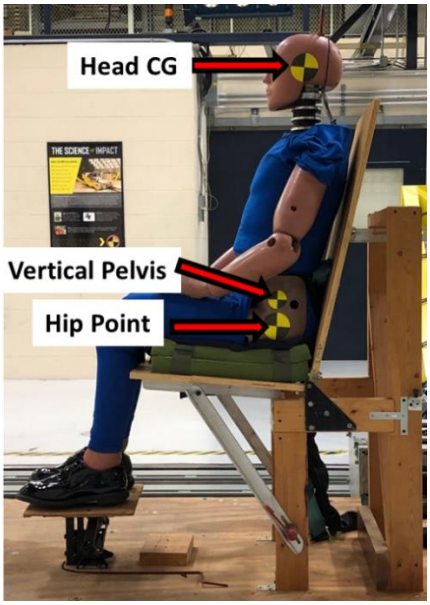

Figure 5: FAA Hybrid III on wooden 1-G seating fixture

Test Pulses

Three different input pulses were used for this test series; however, not every seat was exposed to every pulse (Figure 6). The first two impact pulses are triangular-shaped with 19 G and 30 G peaks, which correspond to the combined horizontal/vertical tests specified in 14 CFR 23.562 (pilot seats) and 27.562/29.562, respectively (Emergency Landing Dynamic Conditions, 2017 14 C.F.R. §25.562, 2022; 14 C.F.R. §27.562, 2022; 14 C.F.R. §29.562; 2022). The third input pulse was a characteristically shaped energy-absorbing (EA) seat pan response from a military helicopter seat designed to control spinal injury risk by stroking when exposed to a vertical impact (Chandler, 1980).

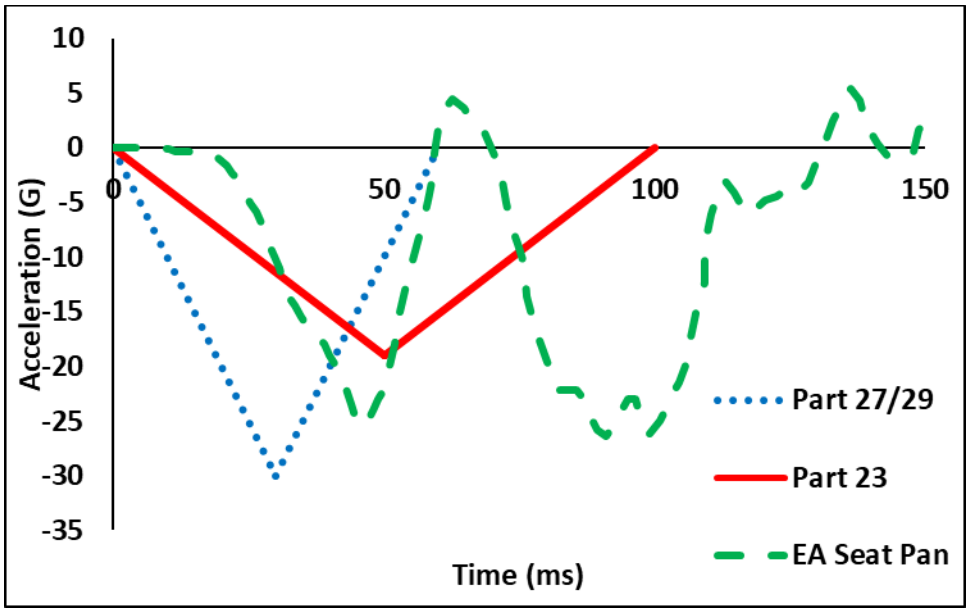

Figure 6: Input acceleration pulses

Instrumentation

Electronic Instrumentation

The instrumentation of the sled, ATD, and seat discussed in this report are shown in Table 1. The full list of channels that were recorded are listed in Appendix A. The test data were gathered and filtered per the requirements of SAE J211-1 (SAE International, 2014). The sign convention of the recorded signals conformed to SAE J1733 (SAE, 2007).

Table 1: Instrumentation list

Description	Units	Filter Class	Bulkhead Mounted	Floor Mounted	Rigid Seat
Sled Acceleration	G	60	X	X	X
Lumbar Force (Fx, Fy, Fz)	lb	600	X	X	X
Pelvis Acceleration (Ax, Ay, Az)	G	1000	X	X	X
Seat Attachment Points Force (Fx, Fy, Fz)	lb	600	X	X	
Seat Pan Acceleration	G	60	X		
Seat Pan Displacement	in	60	X		
Seat Pan Force (Fx, Fy, Fz)	lb	60			X

Video Coverage

High-speed (1000 frames per second), 512 x 1024 resolution color video was captured from each side by cameras aimed perpendicular to the sled (Photron Fastcam SA3, South Central Imaging, Garland, TX, and pco.dimax, PC Tech, Romulus, MI). Targets were placed on the ATD at the head CG, the side of the pelvis at the H-Point, and on a vertical pelvis location. Targets were also placed on rigid structures for scaling and subtracting relative motion between the sled and the camera.

Test Matrix

Nineteen tests were conducted to gather the kinematics and loading data. Table 2 summarizes the variables evaluated for each test in this study. These include the test number, seat type, and the goal peak G for the test.

Table 2: Test matrix

Test Number	Seat Type	Pulse
A17001	Bulkhead-Mounted	30G
A17002	Bulkhead-Mounted	30G
A17003	Bulkhead-Mounted	30G
A17004	Bulkhead-Mounted	30G
A17005	Bulkhead-Mounted	30G
A17006	Bulkhead-Mounted	30G
A18004	Floor-Mounted	19G
A18005	Floor-Mounted	19G
A18009	Floor-Mounted	19G
A18021	Floor-Mounted	19G
A18006	Floor-Mounted	30G
A18007	Floor-Mounted	30G
A18008	Floor-Mounted	30G
A20001	Rigid Seat/ 2” Blue Confor	EA Seat Pan
A20002	Rigid Seat/ 2” Blue Confor	EA Seat Pan
A20003	Rigid Seat/ 2” Blue Confor	EA Seat Pan
A20004	Rigid Seat/ 4” Dax 47	EA Seat Pan
A20005	Rigid Seat/ 4” Dax 47	EA Seat Pan
A20007	Rigid Seat/ 4” Dax 47	EA Seat Pan

RESULTS

Figure 7 shows an example of the achieved pulses for each loading rate.

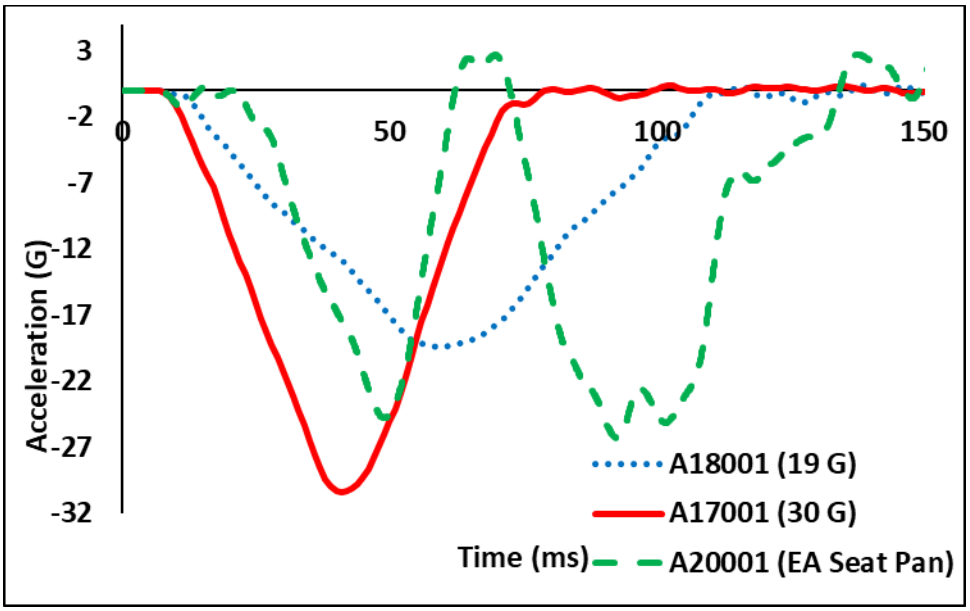

Figure 7: Example of each type of achieved pulses

Kinematics

Figure 8 shows kinematics at 0 ms, 50 ms, 75 ms, and 125 ms for the bulkhead-mounted seat during test A17005, a 30-G test. The frame times selected represented some of the more significant motions of the seat and ATD. The lumbar load in this seat typically peaked at approximately 58 ms. In these tests, the ATD slid down into the seat until the load caused the EA mechanism in the rear of the seat frame to begin to deform (50 ms), allowing the seat to stroke downward (75 ms). Once the seat frame stopped stroking, the ATD began to rotate forward due to the pitch angle of the test condition until the upper torso restraints stopped the motion (125 ms).

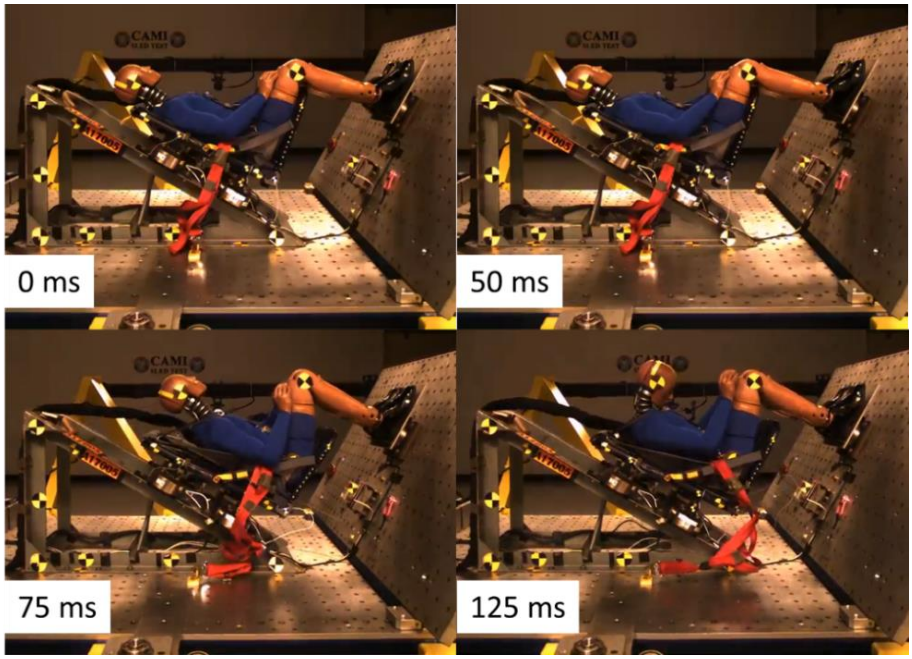

Figure 8: Bulkhead-mounted seat exposed to the 30-G pulse

During the bulkhead-mounted seat tests, repositioning the ATD into the 1-G position changed the distance the seat stroked versus the amount that the seat pan moved (for

additional information, see the Discussion section). Additionally, asymmetrical stroke was noted due to the weight of the ATD instrumentation cable. During the first test, the right side where the cable was routed stroked 2.4 inches, and the left side only stroked 0.8 inches. For the last three tests, the ATD cable was moved to the top center of the seat to reduce this dissymmetry. The last three tests all had a symmetric stroke.

Figure 9 shows kinematics at 0 ms, 50 ms, 75 ms, and 150 ms for the floor-mounted seat during test A18021, a 19-G test. The times selected represented some of the more significant motions of the seat and ATD. The lumbar load in this seat typically peaked at approximately 71 ms. In these tests, the ATD slid down into the seat (50 ms) until the occupant load caused the seat box to buckle and collapse as designed (75 ms). Once the seat base stopped buckling, the ATD began to rotate forward due to the pitch angle of the test condition until the upper torso restraints stopped the motion (150 ms).

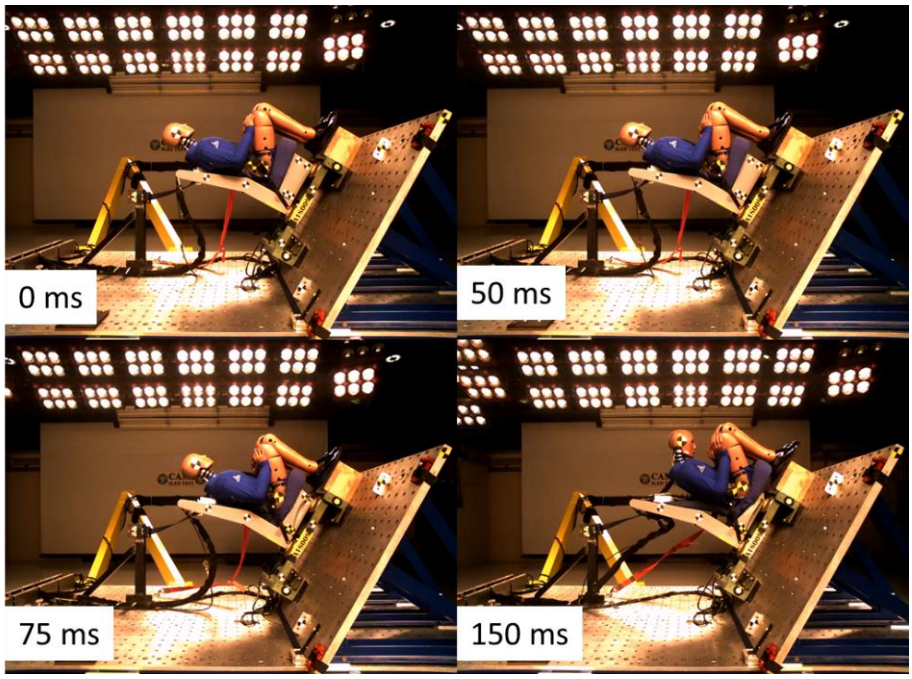

Figure 9: Floor-mounted seat exposed to the 19 G pulse

While the floor-mounted seat is certified for Part 23 aircraft, previous design versions met the more stringent pulse of a Part 27/29 rotorcraft during developmental tests. When the seat was exposed to the 30 G input pulse, a similar downward motion was observed initially, but there was much greater buckling of the front edge of the seat, causing the ATD pelvis to rotate much more in the seat, to the point where submarining would occur (Figure 10). Submarining is when the ATD pelvis has rotated such that the seat belt slides over the pelvis and impinges upon the occupant's abdomen. Submarining would be considered a failure in a certification test. However, in this case, the 30 G pulse is much greater than the seat was required to withstand.

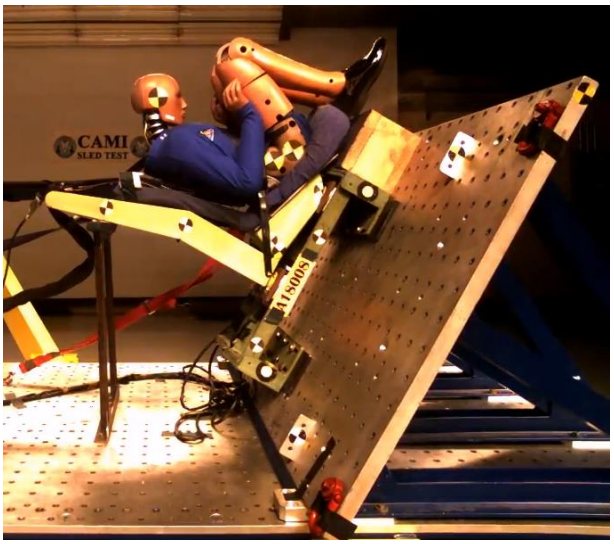

Figure 10: Submarining during 30 G test

Figure 11 shows the kinematics at 0 ms, 50 ms, 66 ms, and 125 ms of the ATD in the rigid seat when using two inches of blue Confor foam and the energy-absorbing seat pan pulse. Similar kinematics were seen in the rigid seat when using the four-inch Dax foam.

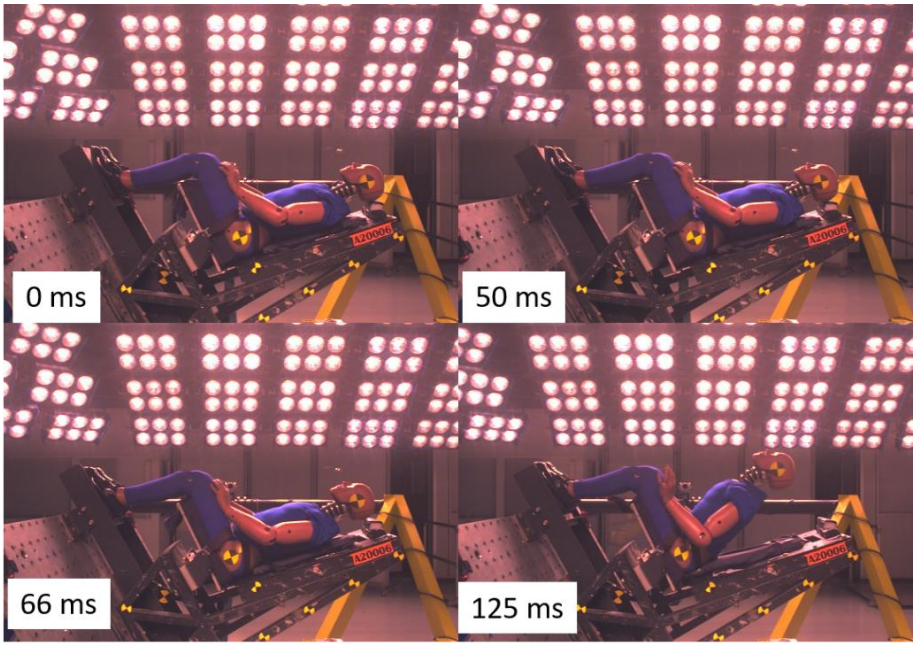

Figure 11: Rigid seat exposed to the EA seat pan pulse

Kinetics

Occupant Loading of Bulkhead-Mounted Seat

Figure 12 shows the bulkhead-mounted seat's representative lumbar load and seat pan displacement time histories. There are no units other than the time on the plot (as well as for Figure 13) to protect the proprietary information of the bulkhead-mounted seat design; however, the plots give a general trend for how these types of seats behave. The load increases until the EA feature begins to deform, or stroke, which causes the load to drop down until the stroke stops, which causes a small plateau in the lumbar load before it further drops as the energy of the impact is dissipated. The seat pan acceleration has one negative peak, which occurs before the sled acceleration peak when the EA mechanism begins to

engage, and three positive peaks. Between the first and second positive peaks, when seat pan acceleration is approximately zero, the lumbar load peaks. This phasing is the intent of a stroking seat to absorb the occupant's energy. The lumbar load then drops to approximately half its value and plateaus as a second positive acceleration occurs. The lumbar load eventually transitions from compression to tension when the third positive seat pan acceleration peak occurs.

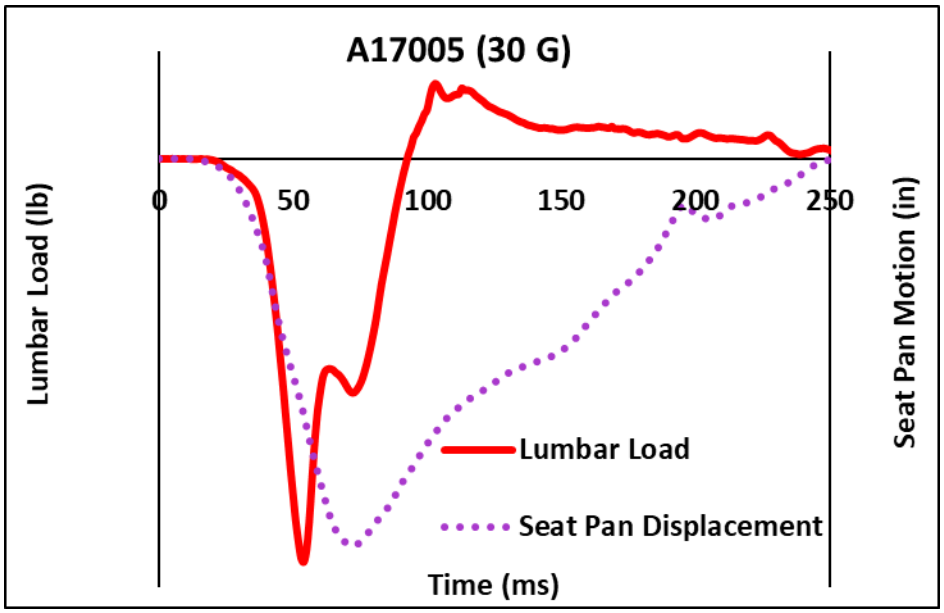

Figure 12: Lumbar load and seat pan displacement

Figure 13 shows a time history of the sum of the four-seat attachment resultant loads and the absolute value of the lumbar load. The lumbar load, by convention, is a negative in this loading scenario as it is compressive. However, to make comparison with the attachment loads easier, the load was inverted for the chart. The load increases for both the lumbar and the attachment points until the EA feature begins to deform. The deformation causes the load at the attachment points to reduce until the stroke of the seat stops, which causes a small plateau in the lumbar load before it further drops as the impact energy is dissipated. The lumbar load follows the same trend as the attachment points, with a slight phase shift and a magnitude of approximately 40% of the total attachment point load throughout the test. The magnitude difference is primarily a function of the difference in weights above the load cells, where the weight of the ATD above the lumbar load cell is approximately 75 lb, while the floor attachment load cells capture the entire ATD weight (approximately 170 lb) and the weight of the seat.

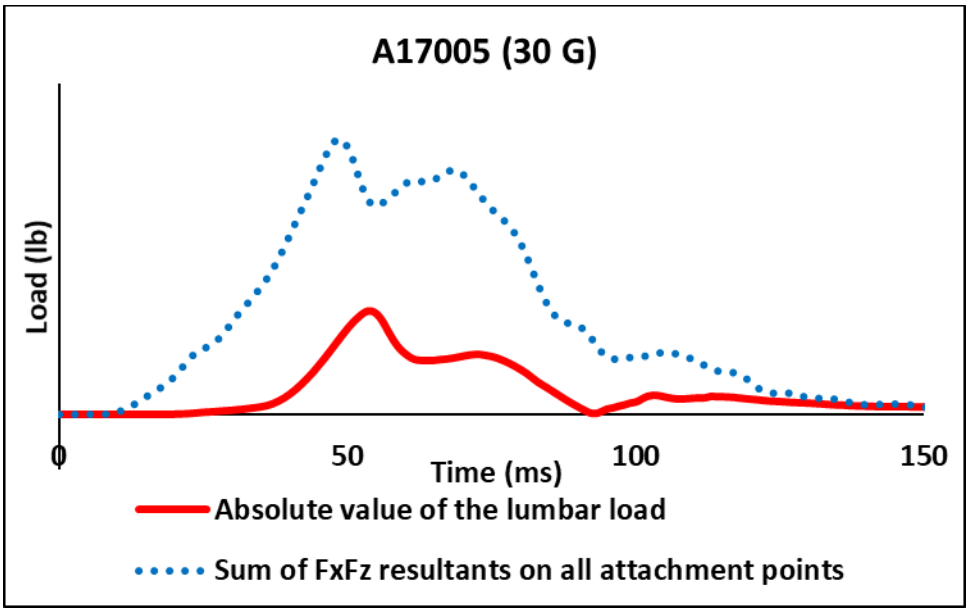

Figure 13: Bulkhead-mounted seat lumbar load magnitude and the sum of the resultant loads on all attachment points

Occupant Loading of Floor-Mounted Seat

Figure 14 shows a representative lumbar load trace for the floor-mounted seat. The load increases until the seat box begins to crumple as designed, then once the seat has fully crumpled, the lumbar load begins to increase again until the remainder of the ATD's energy is dissipated.

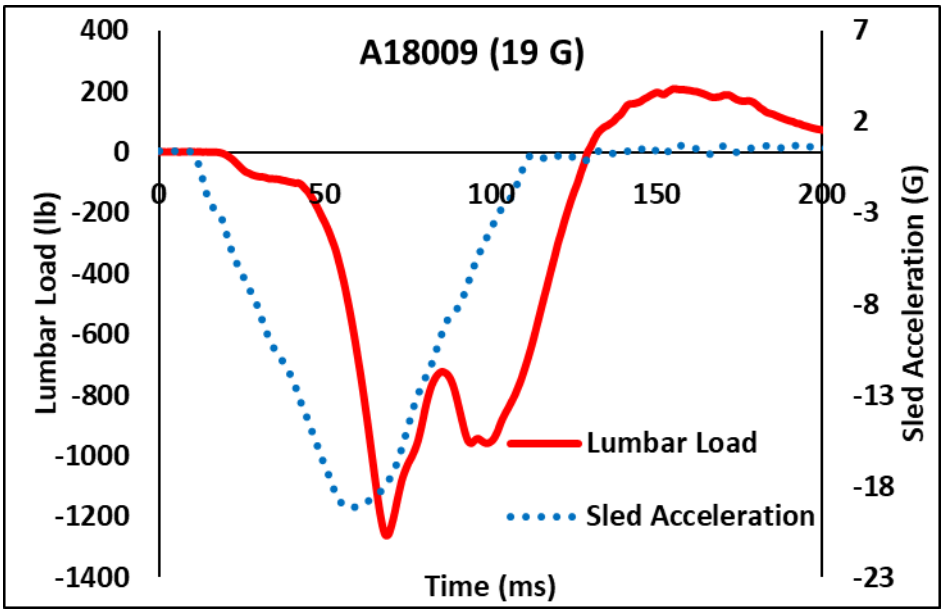

Figure 14: Floor-mounted seat lumbar load and sled acceleration

Figure 15 shows a time history of the sum of the resultant loads and the absolute value of the lumbar load of the floor-mounted seat. The lumbar load, by convention, is a negative in this loading scenario as it is a compressive load; however, to make comparison with the attachment loads easier, the load was made positive on the chart. The load generally increases for the lumbar and the attachment points until the seat begins to crumple. This crumpling causes the load at the attachment points to reduce; once the load into the seat is low enough, the crumpling stops, which causes a small increase in the lumbar load before

it further drops as the energy of the impact is dissipated. The lumbar load follows the attachment point load and is approximately 20% of the attachment load values throughout the impact.

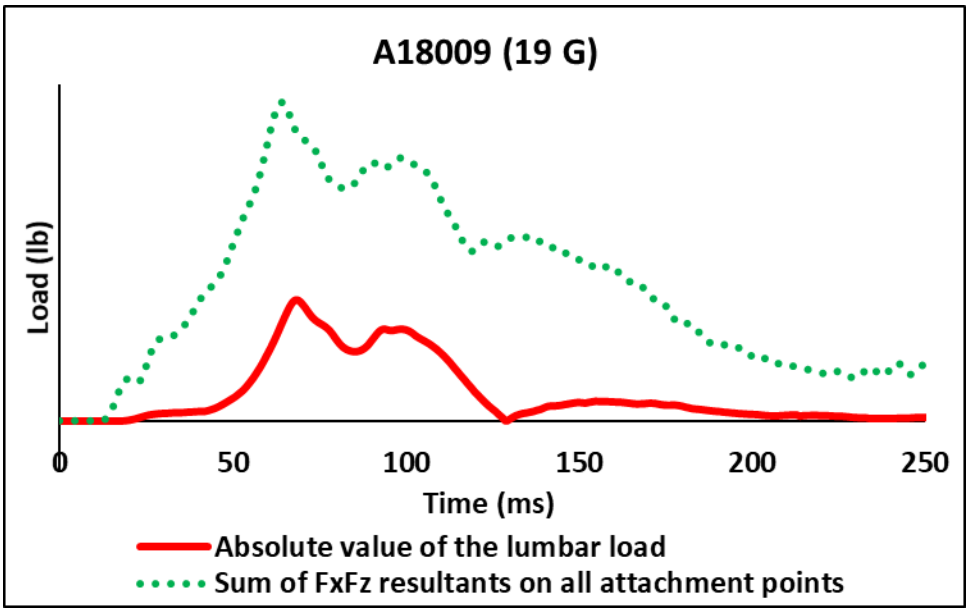

Figure 15: Floor-mounted seat lumbar load magnitude and the sum of the resultant loads on all attachment points

Occupant Loading of EA Seat Pan Pulse

Figure 16 is the time history of the lumbar load of the ATD with Confor foam (A20001), lumbar load with four inches of Dax foam (A20004), and sled acceleration for the rigid seat test using the EA seat pan pulse. All three curves have a double peak. For both cushions, the initial, larger peak occurs when the sled pulse is close to zero acceleration. The Dax cushion produced a higher peak lumbar load than the Confor cushion (three-test average of 2438 lb vs. 2041 lb). Both lumbar loads exceeded the 1500 lb limit.

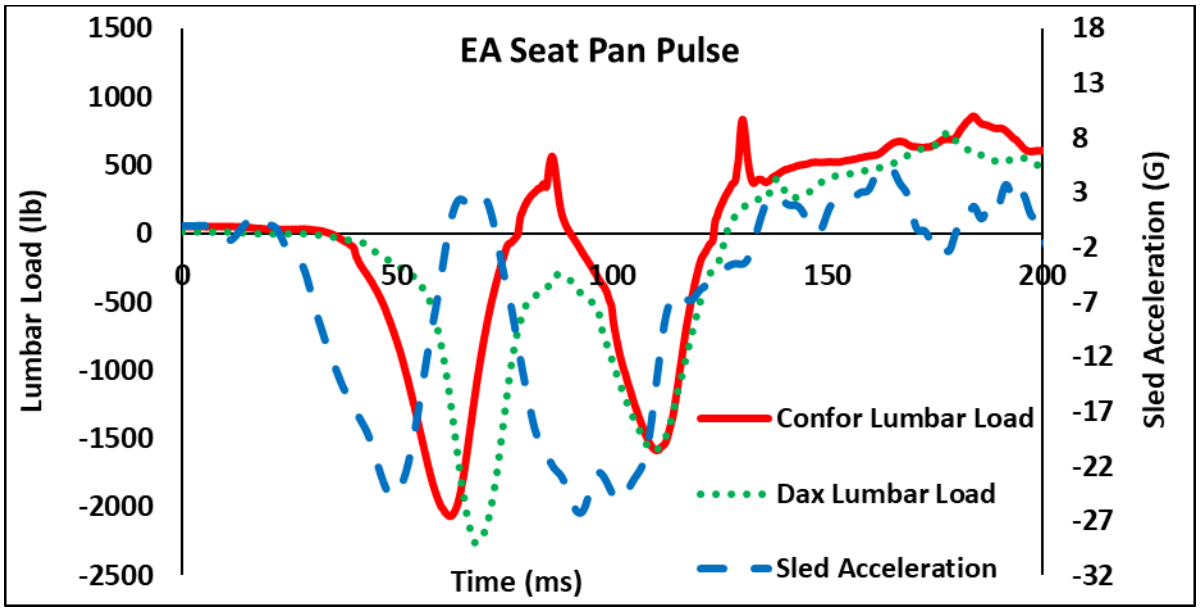

Figure 16: Rigid seat lumbar loads for the two inches of Confor and four inches of Dax lumbar load and sled acceleration

For the historical data, the lumbar load was unavailable; however, pelvis acceleration was. When the historical sled acceleration and pelvis acceleration are overlaid, they are similar in shape (i.e., double peaks), but the seat stroke caused a phase shift resulting in pelvis acceleration peaking when the seat pan acceleration was at the trough between the two peaks (Figure 17). Figure 18 shows the Z-component of the pelvic acceleration for the historical data and representative tests with the Dax and Confor foams.

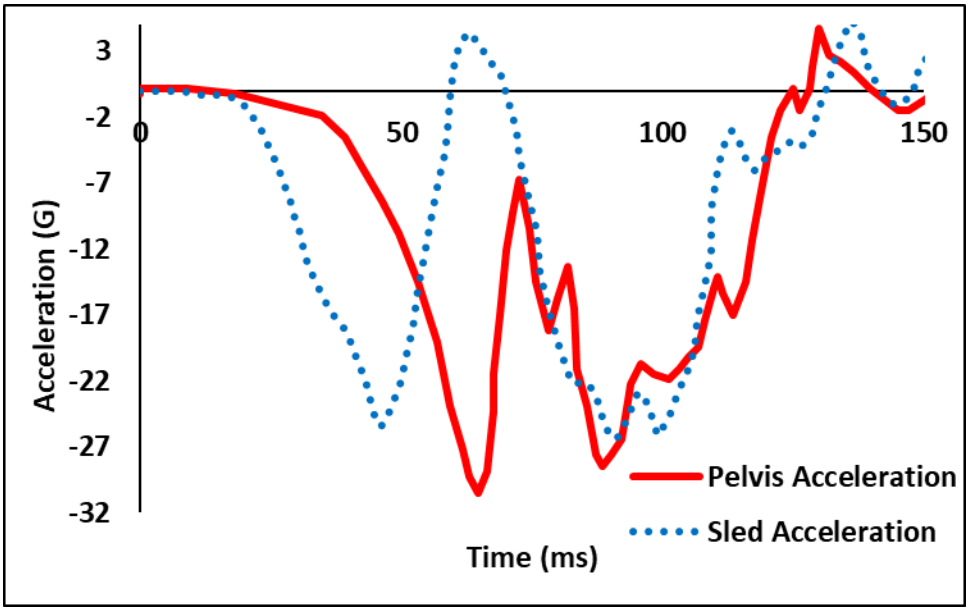

Figure 17: Pelvis and sled acceleration for the historical seat

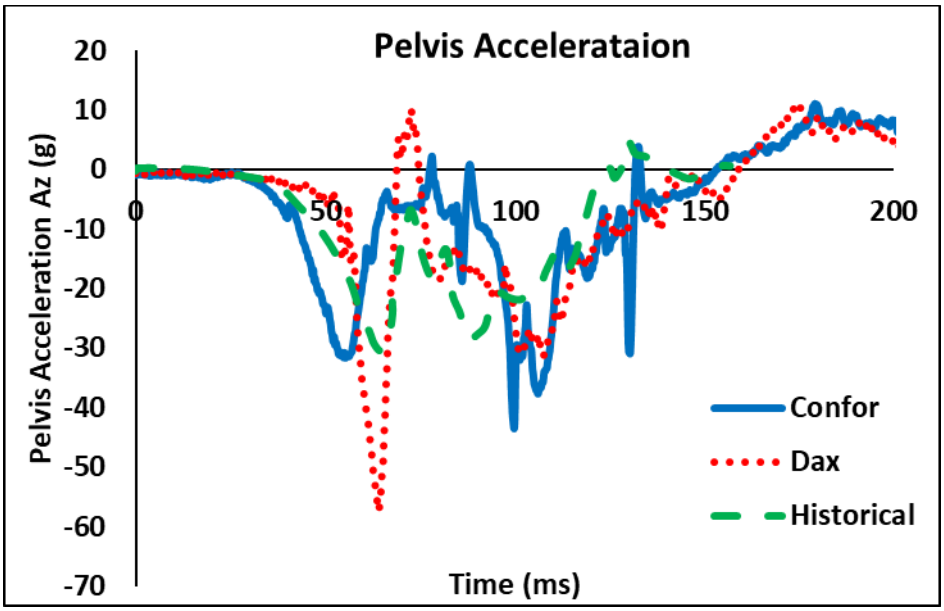

Figure 18: Rigid seat pelvis acceleration for the two inches of Confor, four inches of Dax, and the historical pelvis acceleration

For the Confor test, the timing of the initial pelvic acceleration peak is close to the sled peak (55 ms vs. 50 ms). The magnitude (31.6g) is greater than the 24.5g sled/pan acceleration. For the Dax test, the timing of the initial pelvic peak is close to the sled acceleration peak; however, the peak was much higher (57.4g) than the 25.4g sled/pan acceleration. Additionally, the Confor had two peaks of similar magnitude for the pelvis acceleration like the original test, while the Dax had one peak much larger than the second (approximately double). While the test with Confor produced a similar magnitude as the historical data, the foam used was highly rate sensitive, providing excellent coupling between the occupant and the seat. This foam type is not representative of typical civilian rotorcraft seats, and those seats, which consider comfort in the design, can allow more overshoot than Confor, as occurred with the Dax. Because of this, using a rigid seat representation of the actual seat may not be a suitable replacement for a full-scale test.

DISCUSSION

Lumbar Load, Dynamic Overshoot, and Energy Absorption

The measured load from the lumbar load cell is a function of the ATD weight above the load cell (approximately 75 lbs for a 50th percentile ATD), the component of the sled acceleration in the Z-axis of the load cell (sin 60° = 0.866), and dynamic overshoot from the ATD being uncoupled from the seat. For a combined horizontal-vertical test, the uncoupling is a consequence of the compressibility of the seat cushion and the pelvis foam under the ATD ischial tuberosities and results in the amplification of loads and accelerations transmitted to occupants or structure during impact. Assuming no overshoot, the calculated load for a Part 25 test on a rigid seat is 910 lbs [14 G x 0.866 x 75 lbs]. In a previous research test, the measured load was approximately 940 lbs (DeWeese, 2006). Including a seat cushion can increase this load, ranging from a lumbar load of 1000 lbs for Confor to over 2000 lbs for cushions that allow significant overshoot (DeWeese, Moorcroft, & Taylor, 2021). For a Part 23 pilot seat test, the calculated load without overshoot is 1234 lbs [19 G x 0.866 x 75 lbs], and in practice, loads around 1700 lbs have been measured for rigid seats without cushions (Olivares, 2011). In the 30 G test for rotorcraft, the calculated load without overshoot is 1949 lbs [30 x 0.866 G x 75 lbs]. Test

data are not available for this condition, but assuming a linear relationship between the calculated and measured loads, the measured load would be expected to be approximately 2500 lbs. Any cushion that is added to the rigid seat will increase the measured load due to additional overshoot. Because of this, Part 27/29 seats, as well as most Part 23 seats, must absorb energy to produce a lumbar load below the 1500-lb limit. A simplified estimate of the energy absorbed by the floor-mounted seat can be made by comparing the measured loads of the floor-mounted seat (which includes overshoot from the cushion but absorption from the crushable pan) with the loads expected from a rigid seat without a cushion (Table 3). For the floor-mounted seat, the average measured load was 60 to 70% of the load expected on a rigid seat with no cushion. Thus, the seat pan absorbed a significant amount of energy to reduce the baseline load and account for overshoot from the seat cushion. For the bulkhead-mounted seat, a similar result occurred.

Table 3: Estimated Energy Absorption of the Floor-Mounted Seat

	Calculated Lumbar Load - Rigid Seat without Overshoot	Approximate Lumbar Load - Rigid Seat with Overshoot	Average Measured Lumbar Load of Floor-Mounted Seat	Simplified Energy Absorption Ratio (Approximate / Average)
Part 25	910	940	N/A	N/A
Part 23 Pilot Pulse (19 G)	1234	1700	1229	0.72
Part 27/29 Pulse (30 G)	1949	2500	1469	0.59

ATD Repositioning into the 1-G Location

During testing in the bulkhead-mounted seat, the ATD was placed into the 1-G position and during the first test of the bulkhead-mounted seat, the seat did not stroke as anticipated. The second test was run without placing the ATD into the 1-G position, which allowed the ATD to settle back into the seat, closer to the seat frame (Figure 19). In this second test, the post-test measurement of the seat displacement relative to the rigid frame was closer to what was anticipated. In all bulkhead-mounted tests, the total attachment point loads were higher when the ATD was repositioned into the 1-G position due to the reduced energy absorption from a much lower amount of displacement. Between test A17004 (1-G position) and test A17005 (not repositioned), the difference in peak attachment load was approximately 25% (Figure 20); however, the difference in lumbar loads was less than 10% (Figure 21). Similar changes in lumbar load have been observed in Part 25 testing when the H-point height was not placed in the 1-G position (DeWeese, Moorcroft, & Taylor, 2021).

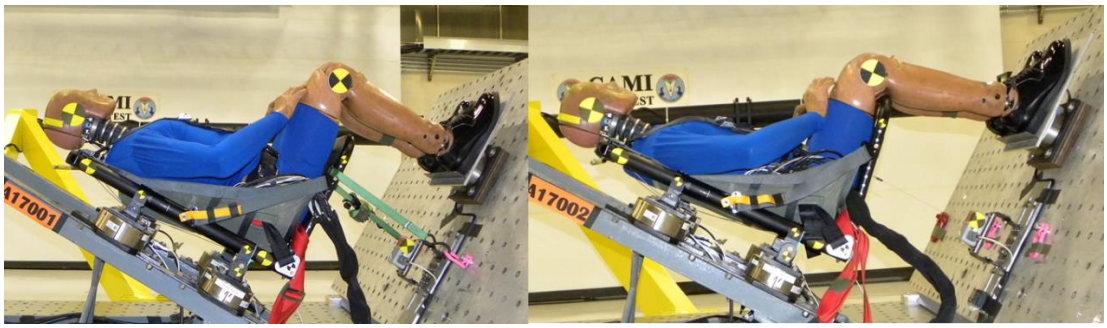

Figure 19: ATD placed in the 1-G position (left) and ATD allowed to settle back into the seat (right)

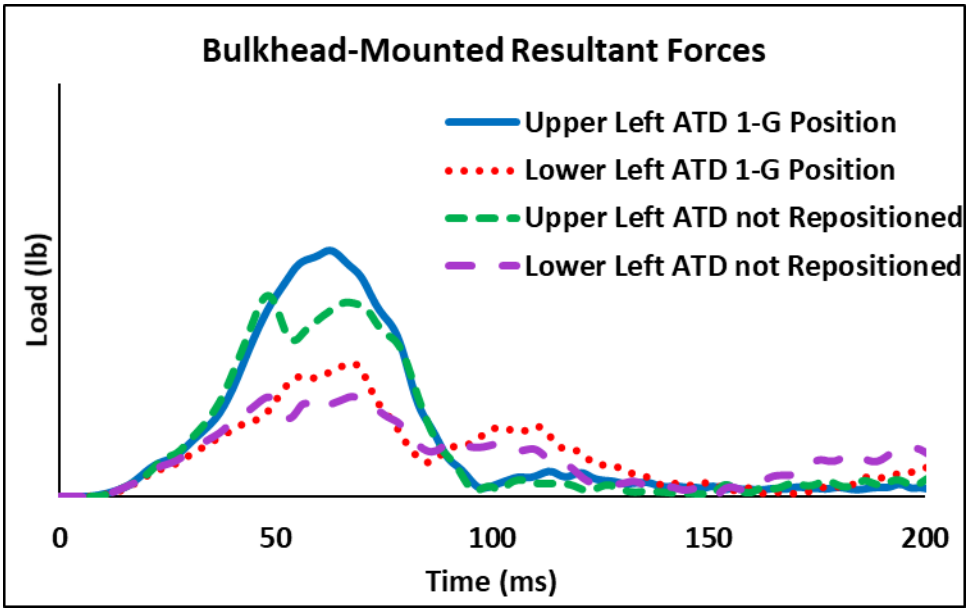

Figure 20: Comparison of the upper and lower left attachment point resultant loads between the ATD repositioned to 1-G and not repositioned

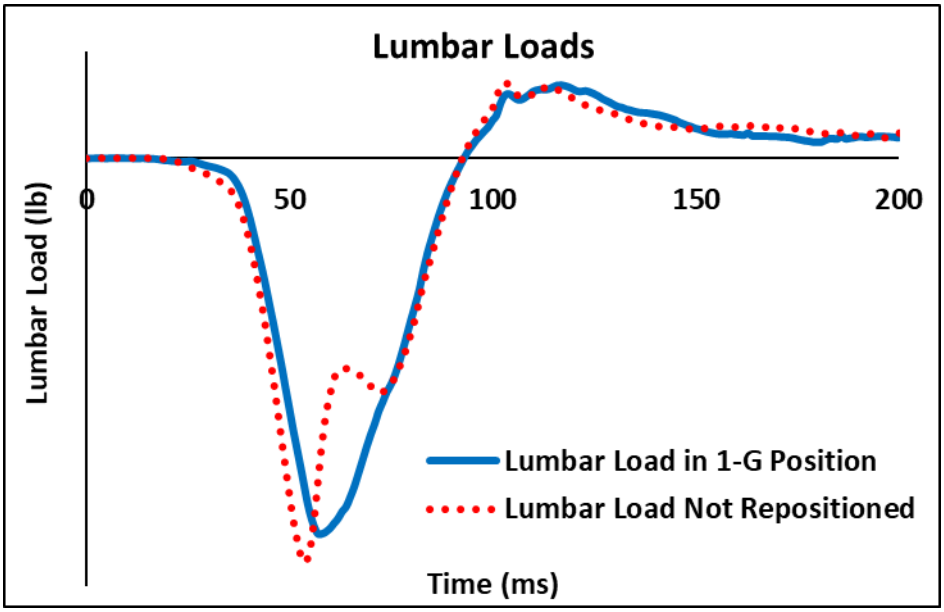

Figure 21: Comparison of lumbar loads between the ATD repositioned to 1-G and not

Instrumentation Cable Routing

While testing the bulkhead seat, ATD instrumentation cable routing became an issue when asymmetric stroking was noted; the right side stroked 2.5 inches, and the left only stroked 0.8 inches. Ideally, the cable would have been routed so that it did not contribute to any stroke, such as out the back through the pan-back intersection; however, there was no way to do that because of the seat's structure. The cable was therefore routed out the top center of the seat back and secured to the structure that held the seat to minimize load transfer while still allowing strain relief (Figure 22).

Figure 22: Instrumentation cable routing: initial (left) and modified (right)

The cable for instrumentation of an ATD is not included in the weight as a part of the certification plan and can exceed 35 lbs. The cable weight depends on how much internal instrumentation is installed in the ATD, so routing can be critical to loading the seat symmetrically. In this test series, the instrumentation cable weighed 12 lbs, approximately 7% of the ATD weight. When exposed to the 30-G input pulse, this adds 312 lbs [12 lbs x 30 G x 0.866] on the seat frame contributing to asymmetric stroke when poorly routed, which can cause additional stroke not representative of the occupant's loading. This is seen in Figure 23, which plots the time history of the resultant of the left and right sides and includes the difference. The additional weight was seen where the maximum divergence between the two sides occurs at approximately 65 ms and is approximately 20% of the total attachment load. The left-right side difference is maintained for the duration of the load plateau. When comparing the time history to a test where the cables were routed out the top and the stroke was symmetric (Figure 24), there can still be some dissymmetry in the loads experienced at the attachment points. In this case, the left and right sides match at the initial peak and the maximum difference is less than 10% of the total attachment loads.

As a best practice, the ATD instrumentation cable should be routed to minimize the effect of the weight on the test performance. Alternatively, ATDs with internal data acquisition systems are becoming more routinely available, which would eliminate this concern, but may impart additional loading to the seat and structure from the weight of the internal hardware (approximately 5 lbs).

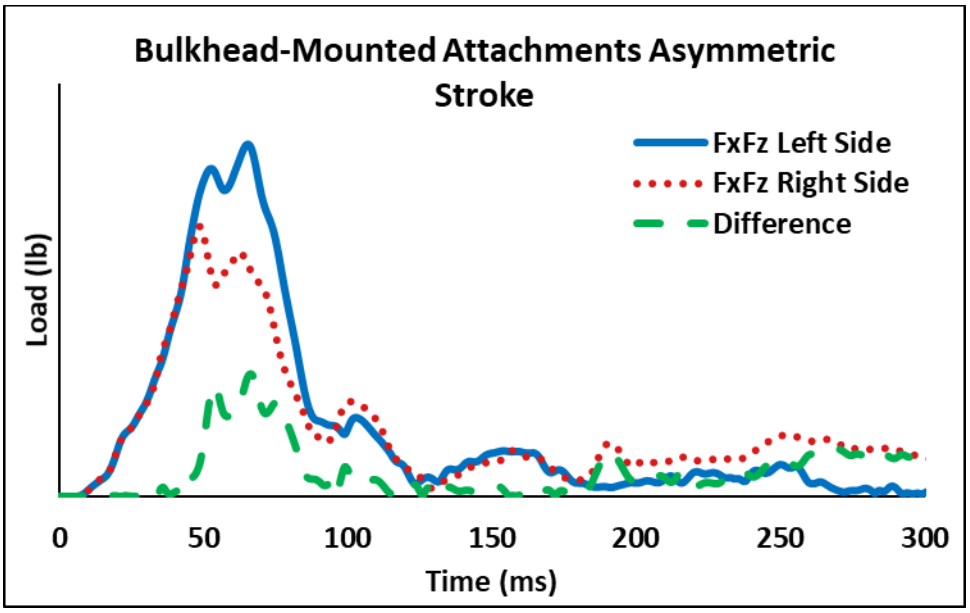

Figure 23: Asymmetric stroke bulkhead-mounted seat attachment point resultant loads for the left and right sides and the difference between them

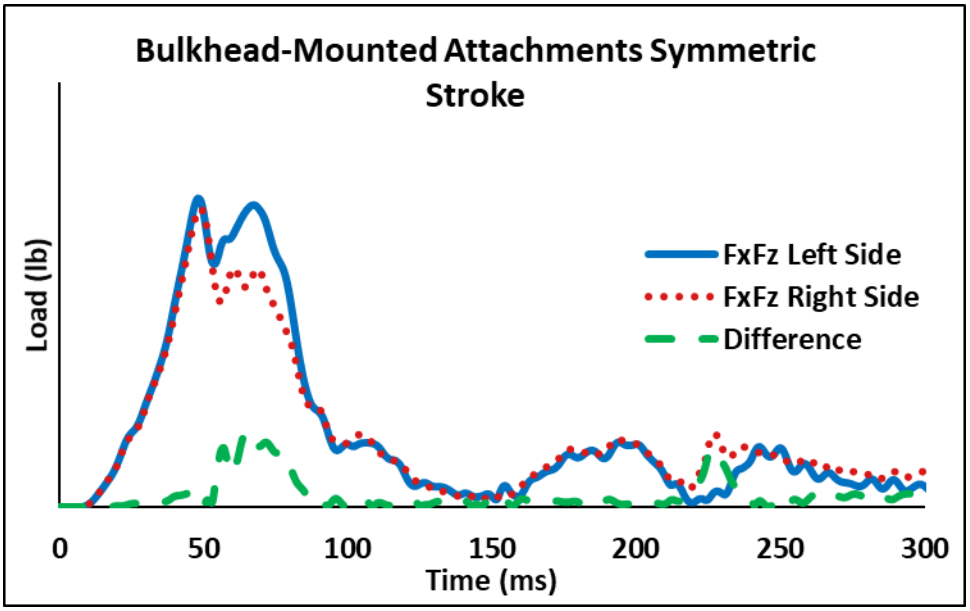

Figure 24: Symmetric stroke bulkhead-mounted seat attachment point resultant loads for the left and right sides and the difference between them

LIMITATIONS

Only two types of real seats were available for assessment in this test series. This did not allow for more comparisons between the types of energy-attenuating seat installations that might be found in aircraft.

For replicating an EA seat pan pulse using a rigid seat, the reference data only included pelvis acceleration, as a lumbar load cell was unavailable at the time of the historical testing. Additionally, only two foams were tested, and both were monolithic. Expanding the evaluation to other foams, buildups, and thicknesses would be necessary to explore the surrogate test method fully.

CONCLUSIONS

The FAA has undertaken research programs to streamline various facets of the certification process. To support this, a project was initiated to evaluate potential methods to qualify replacement elements for worn seat cushions. Part 27 and 29 operate in a high-energy rotorcraft environment, and the seating systems have energy absorption built-in to reduce the occupants' risk of spinal injury. Based on the knowledge gained in research focused on the Part 23 and Part 25 environments, a better understanding of how a seat with energy absorption characteristics behaves during a vertical test is required before any cushion replacement methodology may be considered for Part 27 and 29.

Based on the testing conducted for this research project, the following observations were noted:

- A seat bucket that can stroke during the test absorbs energy by creating a phase shift between the lumbar load and the sled deceleration. The bulkhead-mounted seat accomplished this using a metallic strap that elongated during the test.
- A fixed seat can absorb energy via buckling. The floor-mounted seat accomplished this by designing the seat bottom as a box structure that buckles, acting as a load limiter.
- Both methods of energy absorption were able to reduce the measured lumbar load to below the magnitude expected from a fixed, rigid seat.
- Using a simplified rigid seat test to simulate the seat pan acceleration of a stroking seat may not be a suitable replacement for a full-scale test. While the Confor foam test produced a magnitude similar to the historical data, the phasing was different. Additionally, Confor provides excellent coupling between the occupant and the seat because the foam is highly rate sensitive. The Dax foam, more typical of civilian rotorcraft seat cushions, allowed more overshoot.
- Proper positioning of the ATD is critical to produce representative results. In tests with the bulkhead-mounted seat, differences in peak lumbar load, interface loads, and seat pan displacement were observed between tests with the ATD positioned to match the H-point under 1-G and tests where the ATD was allowed to settle into the seat due to the seat angle. This result agrees with previous testing at CAMI showing differences when the 1-G position is not properly accounted for.
- The instrumentation cable can adversely affect test results depending on the amount of instrumentation included in the ATD. As such, the routing of the cable should be considered when setting up the test to minimize the cable's effect on the loads transmitted into the structure (both in magnitude and symmetry). As a best practice, the ATD instrumentation cable should be routed to minimize the effect of the weight on the test performance.

Combining these results with those from projects focused on Part 23 and Part 25 conditions, which showed that the seat and cushion must be tested as a system, a simplified method of cushion replacement for Part 27/29 rotorcraft is not recommended at this time.

REFERENCES

Chandler, R. (1980). *Dynamic test of joint Army/Navy crashworthy armored crew seat. Memorandum Report AAC-319-80-2*. Federal Aviation Administration, Civil Aeromedical Institute, Protection and Survival Laboratory.

DeWeese R., Moorcroft D., & Taylor A. (2021). *Lumbar Load Variability in Dynamic Testing of Transport Category Aircraft Seat Cushions* (Office of Aerospace Medicine Report, DOT/FAA/AM21-09). Federal Aviation Administration. http://www.tc.faa.gov/its/worldpac/techrpt/ar05-5-1.pdf

DeWeese, R. (2006, August 30). *Measurement of Aircraft Seat Cushion Dynamic Properties and Associated Occupant Lumbar Spine Loads Using Full-scale Sled Tests*. SAE General Aviation Technology Conference; Wichita, KS.

Emergency Landing Dynamic Conditions. 14 C.F.R. §23.562. (2017). https://www.govinfo.gov/app/details/CFR-2017-title14-vol1/CFR-2017-title14-vol1-sec23-562

Emergency Landing Dynamic Conditions. 14 C.F.R. §25.562. (2022). https://www.govinfo.gov/app/details/CFR-2022-title14-vol1/CFR-2022-title14-vol1-sec25-562

Emergency Landing Dynamic Conditions. 14 C.F.R. §27.562. (2022). https://www.govinfo.gov/app/details/CFR-2022-title14-vol1/CFR-2022-title14-vol1-sec27-562

Federal Aviation Administration. (2005). *Policy Statement on Acceptance of a Component Test Method to Demonstrate Compliance with § 25.562(c)(2) for Replacement Seat Bottom Cushions* (Policy Statement No. ANM-115-05-005). https://www.federalregister.gov/documents/2005/04/11/05-7196/policy-statement-on-acceptance-of-a-component-method-to-demonstrate-compliance-with-25562c2-for

Gowdy, V., DeWeese, R., Beebe, M. S., Wade, B., Duncan, J., Kelly, R., & Blaker, J. L. (1999). A lumbar spine modification to the Hybrid III ATD for aircraft seat tests. SAE Technical Paper 1999-01-1609. https://doi.org/10.4271/1999-01-1609

Hooper, S. & Henderson, M. (2005). *Development and Validation of an Aircraft Seat Cushion Component Test – Volume I* (Office of Aerospace Medicine Report DOT/FAA/AR-05/5-1). Federal Aviation Administration. http://www.tc.faa.gov/its/worldpac/techrpt/ar05-5-1.pdf

Moorcroft D., DeWeese R., &Taylor A. (2010, October 25-28). *Improving Test Repeatability and Methods*. The Sixth Triennial International Fire & Cabin Safety Research Conference; Atlantic City, NJ.

Olivares, G. (2011). *Hybrid II and Federal Aviation Administration Hybrid III Anthropomorphic Test Dummy Dynamic Evaluation Test Series* (DOT/FAA/AR-11/24). https://www.tc.faa.gov/its/worldpac/techrpt/ar11-24.pdf

Skandia Inc. (n.d.). Skandia Products and Services Catalog. Davis Junction, IL.

SAE International. (2007). *Sign convention for vehicle crash testing* (SAE Surface Vehicle Information Report No: J1733). Warrendale, PA: SAE International.

SAE International. (2014). *Instrumentation for impact test – Part 1: Electronic instrumentation* (SAE Surface Vehicle Recommended Practice No: J211-1). Warrendale, PA: SAE International.

Taylor A., Moorcroft D., & DeWeese R. (2017, May 9-11). *Comparison of the Hybrid II, FAA Hybrid III, and THOR-NT in Vertical Impacts*. The 73rd Annual American Helicopter Society Forum and Technology Display; Fort Worth, TX.

APPENDIX: Full List of Recorded Channels

Table 4: Full Instrumentation List

Description	Units	Filter Class	Bulkhead Mounted	Floor Mounted	Rigid Seat
Sled Acceleration (main and aux)	G	60	X	X	X
Head Acceleration (Ax, Ay, Az)	G	1000	X		X
Head Rotational Acceleration (Rx, Ry, Rz)	Deg/s	180			X
Upper and Lower Neck Force (Fx, Fy, Fz)	lb	600	X		X
Upper and Lower Neck Moment (Mx, My, Mz)	in-lb	600	X		X
Thorax Acceleration (Ax, Az)	G	180	X		X
Thorax Rotational Acceleration (Rx, Ry, Rz)	Deg/s	180	X		
Thorax Force (Fx, Fy, Fz)	lb	600	X		
Thorax Moment (Mx, My)	in-lb	600	X		
Lumbar Force (Fx, Fy, Fz)	lb	600	X	X	X
Lumbar Moment (Mx, My, Mz)	in-lb	600	X	X	X
Pelvis Acceleration (Ax, Ay, Az)	G	600	X	X	X
Pelvis Rotational Acceleration (Rx, Ry, Rz)	Deg/s	180	X		
Seat Attachment Points Force (Fx, Fy, Fz)	lb	600	X	X	
Floor Force (Fx, Fy, Fz)	lb	600	X		X
Floor Moment (Mx, My, Mz)	in-lb	600	X		
Seat Pan Acceleration	G	60	X		
Seat Pan Displacement	in	60	X		
Seat Pan Force (Fx, Fy, Fz)	lb	60			X
Seat Pan Moment (Mx, My, Mz)	lb	60			X